

# The Mechanism of Electronic Energy Transfer between Excited Mercury ( $^3P_1$ ) Atoms and Gaseous Paraffins

Kang Yang

Contribution from the Central Research Division,  
Research and Development Department, Continental Oil Company,  
Ponca City, Oklahoma. Received April 22, 1967

**Abstract:** Excited mercury atoms in the  $^3P_1$  state react with a paraffin in three different ways: (a) quenching to the metastable state ( $^3P_0$ ), (b) quenching to the ground state ( $^1S_0$ ) with the emission of light, and (c) quenching to the ground state with the rupture of a CH bond. The comparison of quenching rates determined by physical and chemical methods indicates that in the quenching by  $C_2H_6$  and  $C_3H_8$  process c is the major one, while in the quenching by  $C(CH_3)_4$  and  $CH_3CD_2CH_3$  process a predominates. The relative quenching rates between an isotopic pair,  $CH_3CH_2CH_3$ – $CH_3CD_2CH_3$ , hardly change as the temperature is raised from 25 to 202°. This latter observation is used to draw two conclusions: (a) the resonance energy rule is not applicable, and (b) the potential barrier that can be surmounted by thermal motion is not responsible for the isotope effect. In the proposed model of quenching, an excited mercury atom with a definite value of  $J$  is assumed to form a planar complex with a paraffin which is approximated as a diatom, RH. Symmetry arguments indicate that, while the quenching of  $^3P_1$  to  $^1S_0$  is allowed, the quenching of  $^3P_0$  to  $^1S_0$  is forbidden if the product R is in the  $S_g$  state. Available data support this conclusion quite well. Symmetry arguments also indicate that the quenching of  $^3P_1$  to  $^3P_0$  proceeds by the rotational excitation of RH. This is consistent with the observed increase in the metastable atom formation by D substitution. The mean life of the complex is assumed to be governed by two factors: (a) the polarizability of RH, which determines the rate of decomposition of the complex back to reactants, and (b) the CH bond strength, which determines the rate of the decomposition of the complex to HgH and R. This model explains quite well the various differences observed among structurally similar paraffins in the quenching of  $^3P_1$  atoms.

Excited mercury atoms,  $Hg^*(^3P_1)$ , react with paraffins in three different ways: (a) quenching to the metastable state,<sup>1</sup>  $Hg'(^3P_0)$ ; (b) quenching to the ground state with an emission of light;<sup>2</sup> and (c) quenching to the ground state with CH bond rupture.<sup>3</sup> Among structurally similar paraffins, the relative rates of these reactions are fascinatingly different. Thus, metastable atom formation is appreciable in the quenching by  $C(CH_3)_4$  but not in quenching by any other undeuterated paraffins.<sup>1,4,5</sup> In general, deuteration increases the metastable atom formation. This increase is most drastic when the weakest bond, such as the secondary CH in propane, is deuterated.<sup>1</sup> Over-all quenching efficiency increases in the order,  $CH_4 < C_2H_6 < C_3H_8 < i-C_4H_{10}$ , while the light emission from reaction b increases with the reverse order.<sup>2</sup> The efficiency of reaction c is usually reported in terms of the quantum yield,  $\phi(H_2)$ , of hydrogen measured at very low conversions and at very low intensities.<sup>6,7</sup> At atmospheric pressure and room temperature,  $\phi(H_2)$  in methane quenching is nearly zero,<sup>8</sup> while in others it is close to unity.<sup>7</sup> In methane quenching,  $\phi(H_2)$  increases markedly with increasing temperature and decreases with decreasing pressure. In quenching by other paraffins,  $\phi(H_2)$  also decreases with decreasing pressure, this decrease being more pronounced in paraffins with stronger CH bonds.<sup>7</sup> To date, a consistent explanation

of all these variations has not been accomplished. The object of the present work is then to provide some experimental data which help to elucidate these variations and to propose an energy-transfer mechanism on the basis of which various observations can be rationalized.

The first part of the experiment investigates the temperature dependence of the isotope effect between a pair,  $CH_3CH_2CH_3$ – $CH_3CD_2CH_3$ . This is important for two reasons. Previously,<sup>3b</sup> a markedly lower quenching efficiency of  $CH_3CD_2CH_3$  was explained by using absolute rate theory.<sup>9</sup> In this theory, the isotope effect mainly arises because of the difference in the height of the potential barrier that must be surmounted with thermal energy. This difference,  $\Delta E_{1/2}$ , originates from the difference in the zero-point energies of CH and CD bonds and contributes a factor,  $\exp(\Delta E_{1/2}/RT)$ , which governs the magnitude of the isotope effect. Hence, temperature should have a marked effect. It is tempting to suppose the existence of such a barrier, particularly in view of the quantitative agreement between theory and experiment at room temperature. Experimental data, however, show that the predicted temperature dependence is absent. The second reason for investigating the temperature dependence is to test the applicability of the resonance-energy rule in the quenching of  $^3P_1$  atoms to the  $^3P_0$  state. Arguments to be presented later show that the present experimental result is incompatible with this rule.

The second part of the experiment concerns the relative rates of the three reactions mentioned above. Here it is important to note the reported differences<sup>1</sup> in some quenching rates estimated by two different methods. In one method, called the physical method, the quenching cross section ( $\sigma^2_{phys}$ ) is determined rela-

(1) S. Penzes, A. J. Yarwood, O. P. Strausz, and H. E. Gunning, *J. Chem. Phys.*, **43**, 4524 (1965).

(2) S. Penzes, O. P. Strausz, and H. E. Gunning, *ibid.*, **45**, 2322 (1966).

(3) For example, see these reviews: (a) R. J. Cvetanović, *Progr. Reaction Kinetics*, **2**, 39 (1964); (b) H. E. Gunning and O. P. Strausz, *Advan. Photochem.*, **1**, 209 (1964).

(4) A. B. Callear and W. J. R. Tyerman, *Nature*, **202**, 1326 (1964).

(5) A. B. Callear, *Appl. Opt., Suppl.*, **145** (1965).

(6) R. A. Back, *Can. J. Chem.*, **37**, 1834 (1959).

(7) K. Yang, *J. Am. Chem. Soc.*, **86**, 3941 (1964).

(8) R. A. Back and D. Van der Auwer, *Can. J. Chem.*, **40**, 2339 (1962).

(9) S. Glasston, K. Laidler, and H. Eyring, "The Theory of Rate Processes," McGraw-Hill Book Co., Inc., New York, N. Y., 1941.

tive to the rate of fluorescence,  $\text{Hg}^* \rightarrow \text{Hg} + h\nu$ , while in the other method, called the chemical method, the quenching cross section ( $\sigma_{\text{chem}}^2$ ) is determined relative to the reaction  $\text{Hg}^* + \text{N}_2\text{O} \rightarrow \text{Hg} + \text{O} + \text{N}_2$ . For some paraffins, such as  $\text{C}_3\text{H}_8$ , the two cross sections agree quite well, but for those paraffins which show appreciable quenching to the metastable state,  $\sigma_{\text{phys}}^2$  is found to be much larger than  $\sigma_{\text{chem}}^2$ . Using a recent modification of the physical method, we confirm this difference. It is then shown how the relative rates of the three reactions affect the magnitude of the above difference.

The last section treats a model of the collision complex which qualitatively explains why similar paraffins often behave so differently in these energy-transfer reactions.

## Experimental Section

**Material.** Phillips' research grade hydrocarbons and Matheson's nitrous oxide were purified as described before.<sup>10</sup> Deuteriopropane from Merck Sharp and Dohme Co., Ltd. (Montreal, Canada) was passed through a  $\text{H}_2\text{SO}_4\text{-P}_2\text{O}_5$  mixture to remove olefins and through a KOH trap to remove any acid spray. It was then thoroughly degassed.

**Physical Method.** The quenching of mercury fluorescence was investigated using equipment described previously<sup>11</sup> with a modification that the temperature of the fluorescence cell was kept within  $\pm 1^\circ$  at different temperatures, using a heater inserted in an aluminum block surrounding the cell. As before, the temperature of the mercury reservoir was kept within  $\pm 0.1^\circ$  using an ethylene glycol bath. Table I shows an example of experimental data.

**Table I.** The Quenching of Mercury Fluorescence by  $\text{CH}_3\text{CD}_2\text{CH}_3^a$

$p$ , torr	$Q'_0$	$Q'$
0.504	101.0	86.5
0.576	100.8	85.0
0.684	100.7	81.8
0.720	100.0	80.6
0.772	99.1	76.4
0.792	101.0	80.8
1.33	101.0	71.5
1.66	100.2	66.3
2.45	100.0	59.9
3.49	99.2	51.5

<sup>a</sup> Cell temperature,  $25^\circ$ ; mercury reservoir temperature,  $20^\circ$ ;  $Q'_0$  and  $Q'$  denote photocurrents (arbitrary unit) in the absence and presence of  $\text{CH}_3\text{CD}_2\text{CH}_3$ .

**Chemical Method.** The equipment used in the determination of the quantum yield of nitrogen in the mercury-sensitized photolysis of  $\text{N}_2\text{O-M}$  systems was the same as before<sup>10</sup> except that the Vycor cell was placed in a temperature-controlling box equipped with a fan, heater, and quartz window. Nitrogen was analyzed using a Porapak Q column at room temperature with helium as a carrier gas. Both the stability and the sensitivity of this column were superior to the charcoal-molecular sieve column used in our earlier study. At room temperature, the column would not separate nitrogen from oxygen; but oxygen was absent in the present experiment. Nitrous oxide, which was not absorbed irreversibly, was backflushed as before. Both the plot of peak height against nitrogen pressure and the plot of peak height against irradiation time were good straight lines passing through the origin. Other details of similar experiments were described before.<sup>7,10,11</sup> Table II shows an example of experimental data.

## Results

(A) **Temperature Dependence of Isotope Effect.** It is convenient to report the results of the quenching

(10) K. Yang, *J. Am. Chem. Soc.*, **87**, 5294 (1965).

(11) K. Yang, *ibid.*, **88**, 4575 (1966).

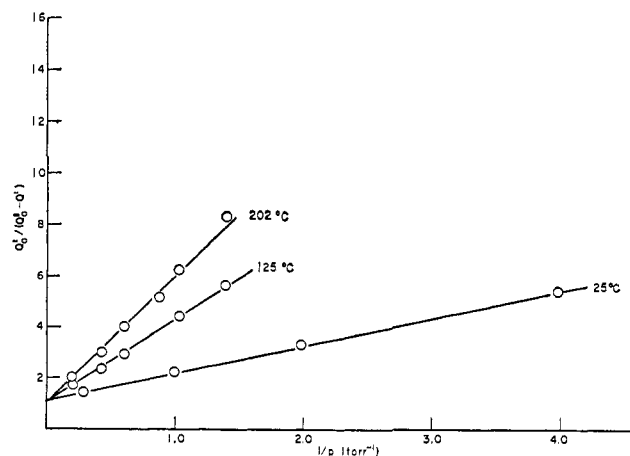


**Figure 1.** The quenching of fluorescence by propane at  $t_{\text{res}} 20^\circ$  and at various temperatures of the fluorescence cell.

experiments using the equation

$$\frac{Q'_0}{Q'_0 - Q'} = \alpha + \beta[M]^{-1} \quad (\text{I})$$

where  $Q'_0$  and  $Q'$  are photocurrents in the absence and presence of M, while  $\alpha$  and  $\beta$  are constants independent of  $[M]$ . As shown later, the ratio  $\alpha/\beta$  is proportional to the rate constant of the quenching. According to (I), the plot of  $Q'_0/(Q'_0 - Q')$  against  $[M]^{-1}$  should be a straight line. Such plots are shown in Figure 1 for  $\text{CH}_3\text{CH}_2\text{CH}_3$  and in Figure 2 for  $\text{CH}_3\text{CD}_2\text{CH}_3$ . These

**Table II.** Nitrogen Formed at Various  $[\text{C}_3\text{H}_8]/[\text{N}_2\text{O}]^a$

$[\text{C}_3\text{H}_8]/[\text{N}_2\text{O}]$	$[\text{N}_2]$ , torr	$\phi$
1.00	0.232	0.914
2.08	0.214	0.843
3.00	0.209	0.823
5.15	0.175	0.690
7.00	0.159	0.626
8.10	0.148	0.583
9.00	0.138	0.544
10.40	0.137	0.540
12.30	0.133	0.524
15.00	0.119	0.469
25.70	0.0954	0.376
49.00	0.0695	0.274
65.70	0.0604	0.238
79.00	0.0563	0.222
99.00	0.0487	0.192

<sup>a</sup> Total pressure, 400 torr; irradiation time, 10 min; cell temperature,  $28 \pm 2^\circ$ ; mercury reservoir temperature,  $20 \pm 0.2^\circ$ ; intensity, 0.0254 torr/min.

data were obtained at a constant mercury reservoir temperature of  $20^\circ$  and at various temperatures of the fluorescence cell. Table III summarizes the ratio  $\alpha/\beta$  obtained by a least-squares method. With increasing

**Table III.** The Relative Rate Constant of Quenching at Different Temperatures

Temp, $^\circ\text{C}$	$\alpha/\beta$ , torr $^{-1}$		$(\alpha/\beta)_\text{H}/(\alpha/\beta)_\text{D}$
	$\text{C}_3\text{H}_8$	$\text{C}_3\text{H}_6\text{D}_2$	
25	1.04	0.361	2.88
125	0.356	0.128	2.78
202	0.224	0.0835	2.68

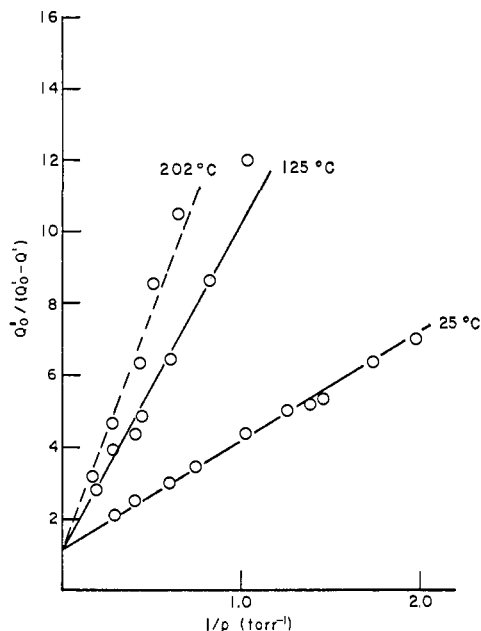


Figure 2. The quenching of fluorescence by  $\text{CH}_3\text{CD}_2\text{CH}_3$  at  $t_{re}^0$  20° and at various temperatures of the fluorescence cell.

temperature,  $\alpha/\beta$  sharply decreases (see Appendix), but the ratio of the two  $\alpha/\beta$  values for the isotopic pair shows very little, if any, temperature dependence.

**(B) Absolute Quenching Rates.** In the determination of quenching rates by the physical method, two opposing factors must be compromised. The pressure of M should be low so that the collision broadening of the absorption line can be neglected. Otherwise, the amount of light absorbed by Hg atoms depends on the pressure of M and a meaningful interpretation of the quenching data becomes very difficult.<sup>7</sup> On the other hand, the pressure of M must be high enough to quench the fluorescence appreciably, so that the difference,  $Q'_0 - Q'$ , can be measured accurately. At a given pressure of M, more light is quenched when the mercury vapor pressure is high.<sup>11</sup> Hence, it is desirable to employ a higher pressure of mercury in an investigation of a compound having a lower quenching rate. In the present work,  $\alpha/\beta$  for  $\text{CH}_3\text{CH}_2\text{CH}_3$  is measured relative to that for  $\text{C}_2\text{H}_4$  (whose absolute cross section is known to be  $48.2 \text{ \AA}^2$ ) at a mercury reservoir temperature,  $t_{res}$ , of 16°. For  $\text{CH}_3\text{CD}_2\text{CH}_3$  and  $\text{C}(\text{CH}_3)_4$ ,  $\alpha/\beta$  is determined relative to  $\alpha/\beta$  for  $\text{CH}_3\text{CH}_2\text{CH}_3$  at  $t_{res}$  20°, while  $\alpha/\beta$  for  $\text{C}_2\text{H}_6$  and  $\text{C}(\text{CH}_3)_4$  are compared at  $t_{res}$  25°. Results are summarized in Table IV. The quenching rate follows the order:  $\text{C}_2\text{H}_4 > \text{C}_3\text{H}_3 > \text{C}(\text{CH}_3)_4 > \text{CH}_3\text{CD}_2\text{CH}_3 > \text{C}_2\text{H}_6$ .

Table IV. Constants in the Modified Stern-Volmer Formula<sup>a</sup>

Quencher	Reservoir temp, °C	$\alpha/\beta$ , torr <sup>-1</sup>
$\text{C}_2\text{H}_4$	16.1	13.2
$\text{C}_3\text{H}_3$	16.1	0.489
$\text{C}_3\text{H}_3$	20.0	1.04
$\text{CH}_3\text{CD}_2\text{CH}_3$	20.0	0.361
$\text{C}(\text{CH}_3)_4$	20.0	0.734
$\text{C}_3\text{H}_3$	25.0	3.37
$\text{C}_2\text{H}_6$	25.0	0.693

<sup>a</sup> Equation 1 in text, at a constant cell temperature of 25° and at different mercury reservoir temperatures.

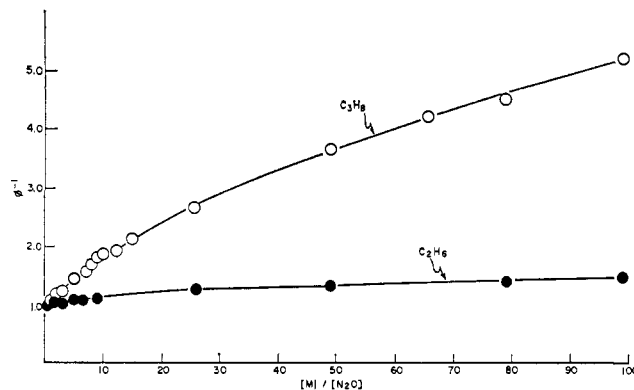
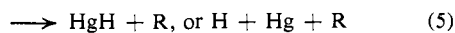
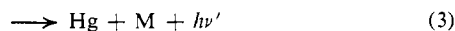
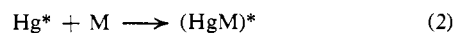
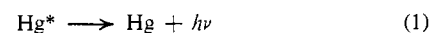
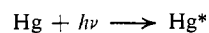


Figure 3. Quantum yield,  $\phi$ , of nitrogen at various  $[M]/[\text{N}_2\text{O}]$ , in  $\text{CH}_3\text{CH}_2\text{CH}_3\text{-N}_2\text{O}$  and  $\text{CH}_3\text{CH}_3\text{-N}_2\text{O}$  systems.

**(C) Chemical Method.** The results on the quantum yield,  $\phi$ , of nitrogen are reported by plotting  $\phi^{-1}$  against  $X$  ( $= [M]/[\text{N}_2\text{O}]$ ), as is usually done. As shown in Figures 3 and 4, the plot is linear if  $X$  is not too large. This linearity is expected if  $\text{Hg}^*$  undergoes a simple competitive reaction with  $\text{N}_2\text{O}$  and M. The slopes of the linear portion agreed well with literature values.<sup>3,10</sup> At high  $X$  values, the plot curves down markedly both in  $\text{CH}_3\text{CH}_2\text{CH}_3$  and  $\text{C}(\text{CH}_3)_4$ . It should be noted that, if one considers the data only at high  $X$  values, the plot is apparently linear, but the intercept is higher than unity and the slope is lower. In the  $\text{C}_2\text{H}_6\text{-N}_2\text{O}$  system, the decrease in  $\phi$  even at high  $X$  is very small. Because of this, even though the slope at high  $X$  values was somewhat lower than at lower  $X$ , we could not reach a definite conclusion (see Figure 3). Figure 5 shows a similar plot for the  $\text{CH}_3\text{CD}_2\text{CH}_3\text{-N}_2\text{O}$  system at 25 and 150°. The intercept here may be slightly higher than unity. For a definite conclusion, more experimental data are needed. It is clear, however, that the temperature dependence of  $\sigma^2_{chem}$  is negligible.

## Discussion

**(A) Physical Method.** The results of quenching experiments are explainable with the following mechanism



where  $\nu'$  denotes the light other than the resonance line, and  $\text{M}'$  denotes rotationally or vibrationally excited species. The major modification of the previous mechanism is the inclusion of (3), which is shown to be important.<sup>2</sup> This modification considerably alters the rate equation. We suppose that the sensitivity of the photomultiplier tube is the same at  $\nu$  and  $\nu'$ ; then the resulting rate equation is

$$\frac{Q_0}{Q} = \frac{1 + (k_2/k_1)\tau_c(k_3 + k_4 + k_5)[M]}{1 + (k_2/k_1)\tau_c k_3[M]} \quad (II)$$

where  $Q_0$  and  $Q$  denote the intensity of the light ( $\nu$

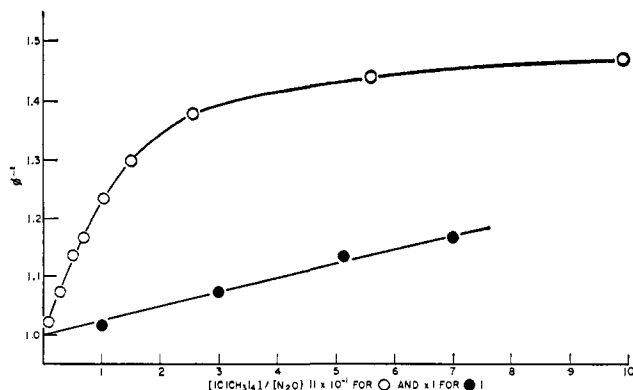


Figure 4. Quantum yield,  $\phi$ , of nitrogen at various  $[M]/[N_2O]$  in  $C(CH_3)_4-N_2O$  systems.

+  $\nu'$ ) in the absence and presence of  $M$ ,  $k_i$  is the rate constant of  $i$ th reaction, and  $\tau_c$  is the mean life of the collision complex defined

$$1/\tau_c = k_{-2} + k_3 + k_4 + k_5$$

Most of the experimental data are obtained at less than 50% quenching; hence,  $(k_2/k_1)\tau_c k_3[M] < 1$ . We then expand the reciprocal of the denominator and retain the terms up to the first power of  $M$

$$\frac{Q_0}{Q} = 1 + \frac{k_2}{k_1}\tau_c(k_4 + k_5)[M] \quad (\text{III})$$

This is the Stern-Volmer formula in which  $k_2$  is replaced by  $k_2\tau_c(k_4 + k_5)$ . Experimental photocurrents,  $Q'_0$  and  $Q'$ , contain a contribution from stray light,  $\Delta$ ; hence,  $Q'_0 = Q_0 + \Delta$  and  $Q' = Q + \Delta$ . To take into account the effect of imprisonment,  $k_1$  is replaced by  $ck_1$  ( $c < 1$ ), as before.<sup>10</sup> With these modifications, (III) at once yields the modified Stern-Volmer formula (I), where  $\alpha = [1 - (\Delta/Q_0)]^{-1}$  and

$$\alpha/\beta = k_2\tau_c(k_4 + k_5)/(ck_1) \quad (\text{IV})$$

The imprisonment correction factor,  $c$ , in (IV) depends on the geometry of the cell and the pressure of mercury but not on the nature of the quencher. Hence, the ratio of the two  $\alpha/\beta$  values between the pair  $CH_3CH_2CH_3-CH_3CD_2CH_3$  in Table III represents the isotope effect in  $k_2\tau_c(k_4 + k_5)$  values. It is now necessary to define  $\sigma^2_{phys}$  as

$$k_2\tau_c(k_4 + k_5) = \sigma^2_{phys}(8\pi RT/\mu)^{1/2} \quad (\text{V})$$

For ethylene,  $\sigma^2_{phys} = 48.2 \text{ A}^2$ . The use of this value together with the data in Table IV gives various  $\sigma^2_{phys}$  as summarized in Table V. Although relative  $\sigma^2_{phys}$  values agree reasonably with published results,<sup>3</sup> the absolute values are much larger. This is due to the fact

Table V. Quenching Cross Sections Estimated by Physical and Chemical Methods

Quencher	$\sigma^2_{phys}$ , A <sup>2</sup>	$\sigma^2_{chem}$ , A <sup>2</sup>
$C(CH_3)_4$	1.9	0.8
$CH_3CD_2CH_3$	0.8	0.3
$CH_3CH_3$	0.4	0.3
$CH_3CH_2CH_3$	2.2	2.4
$CH_2=CH_2$	48.2	48.2 <sup>a</sup>

<sup>a</sup> Assumed value; see ref 11.

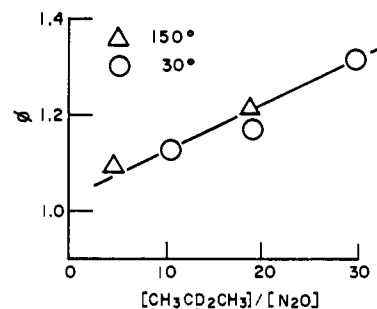
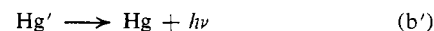
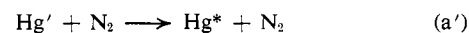


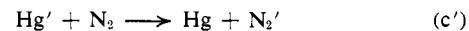
Figure 5. Quantum yield,  $\phi$ , of nitrogen at various  $[M]/[N_2O]$  in  $CH_3CD_2CH_3-N_2O$  systems.

that, while the published data are based on a theoretical  $c$  value, the present work employs an experimentally determined  $c$  value.<sup>11</sup>

In the quenching with nitrogen,<sup>12</sup> the rate equation is much more complicated because  $Hg'$  atoms contribute to photocurrent through the reactions

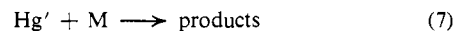
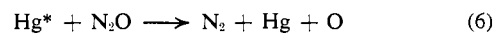


In this case, the competing reaction



is very slow,  $k_c = 4.7 \text{ mm}^{-1} \text{ sec}^{-1}$  at 25°. Available rate data<sup>5</sup> together with some reasonable approximations indicate that in the present experiments quenching reactions corresponding to reaction  $c'$  are several orders of magnitude faster. Thus, under the experimental conditions where (III) is valid,  $Hg'$  atoms are not likely to contribute significantly to photocurrent.

(B) Chemical Method. In the presence of  $N_2O$ , in addition to reactions 1-5, reactions 6-8 should be considered



The occurrence of reaction 6 is well known,<sup>3a</sup> while the occurrence of reaction 8 is at present a reasonable presumption. In  $N_2O$  quenching, the quenching cross section is very high, indicating that  $k_{-2} \simeq 0$ . Metastable atoms are not detected here; thus  $k_4 \simeq 0$ . Also,  $k_3$  is likely to be nearly zero because compounds having large cross sections, such as  $NO$  and  $C_2H_4$ , show no light emission. Hence, the decomposition of the complex,  $(HgN_2O)^*$ , is not considered explicitly. At high total pressure of quenchers, the rate of reaction 1 is negligible, and the rate equation for the quantum yield of nitrogen is readily obtained (eq VI). Since  $k_2/k_6 \ll 1$ , and very

$$\phi^{-1} = \frac{1 + \{(k_7/k_8) + (k_2/k_6)\tau_c(k_3 + k_4 + k_5)\}X + \frac{(k_2/k_6)(k_7/k_8)\tau_c(k_3 + k_4 + k_5)X^2}{1 + \{(k_7/k_8) + (k_2/k_6)\tau_c k_4\}X}}{1 + \{(k_7/k_8) + (k_2/k_6)\tau_c k_4\}X} \quad (\text{VI})$$

likely  $k_7/k_8 \ll 1$ , the reciprocal of the denominator can be expanded at not too large  $X$ . Retaining up to the first power of  $X$ , we obtain

$$\phi^{-1} = 1 + (k_2/k_6)\tau_c(k_3 + k_5)X \quad (\text{VII})$$

The form of this equation is the same as the one em-

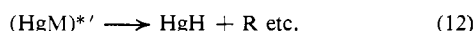
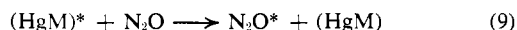
(12) J. E. McAluff and D. J. LeRoy, *Can. J. Chem.*, 43, 2279 (1965).

ployed previously,<sup>3</sup> but the meaning of the cross section now becomes modified as

$$k_2\tau_c(k_3 + k_5) = \sigma^2_{\text{chem}}(8\pi RT/\mu)^{1/2} \quad (\text{VIII})$$

At low  $X$  values, (VII) is well satisfied, and the slopes together with the known  $\sigma^2_{\text{chem}}$  value of 27 Å<sup>2</sup> for N<sub>2</sub>O provide  $\sigma^2_{\text{chem}}$  values for various paraffins as summarized in Table V.<sup>13</sup> Here again, relative values agree well with previous work, but absolute values are higher because a higher value of  $\sigma^2_{\text{chem}}$  for N<sub>2</sub>O is employed.<sup>11</sup>

At high  $X$  values, the  $\phi^{-1}$  vs.  $X$  plot curves down markedly, indicating that some excess nitrogen other than that due to reaction 6 is formed. According to the present mechanism, reaction 8 supplies this nitrogen, but this cannot be the sole source because, in propane quenching where  $k_3 \simeq 0$ , the excess nitrogen is also appreciable at high  $X$  values. Probable reactions are



A basic assumption here is that the complex lives long enough to undergo collisional processes when  $[\text{M}]$  and  $[\text{N}_2\text{O}]$  are high. Reactions 11 and 12 are consistent with decreasing  $\phi(\text{H}_2)$  with decreasing  $[\text{M}]$ . Much more extensive data than those given here are needed to prove or disprove the occurrence of these reactions. In the present work, the possible occurrence of these reactions is neglected, hoping that the limiting equation (VII) remains substantially unaltered.

**(C) Comparison of the Two Cross Sections.** Table V shows that the cross sections estimated by the two methods agree well in C<sub>3</sub>H<sub>8</sub> quenching and probably also in C<sub>2</sub>H<sub>6</sub> quenching but not in C(CH<sub>3</sub>)<sub>4</sub> or in CH<sub>3</sub>-CD<sub>2</sub>CH<sub>3</sub> quenching. This confirms previous work.<sup>1</sup> From (V) and (VIII)

$$\frac{\sigma^2_{\text{phys}}}{\sigma^2_{\text{chem}}} = \frac{k_4 + k_5}{k_3 + k_5} \quad (\text{IX})$$

If  $k_5$  is much larger than  $k_4$  or  $k_3$ , the two cross sections agree. Since  $\sigma^2_{\text{phys}} > \sigma^2_{\text{chem}}$  in C(CH<sub>3</sub>)<sub>4</sub> and CH<sub>3</sub>-CD<sub>2</sub>CH<sub>3</sub> quenching, we conclude that here  $k_4 > k_3$ . The numerical values in Table V also indicate that  $k_4 \geq k_3$ . This is consistent with experimental observations that detectable Hg' atoms are formed in those quenchings where  $\sigma^2_{\text{phys}} > \sigma^2_{\text{chem}}$ .

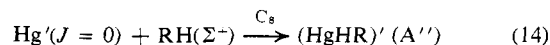
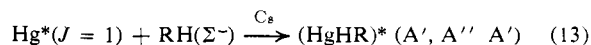
**(D) The Collision Complex and Quenching Mechanism.**

In considering the quenching mechanism, it is important to note several facts which indicate that, in mercury, spin-orbit coupling is very strong and the total angular momentum quantum number  $J$  is the only reliable quantum number. The transition,  $^3\text{P}_1 \rightarrow ^1\text{S}_0$ , occurs readily even though the spin selection rule is violated, while the transition,  $^3\text{P}_0 \rightarrow ^1\text{S}_0$ , which violates the  $J$  selection rule, is forbidden. The quenching of Hg\* atoms to the ground state by CO occurs<sup>5</sup> with high efficiency in spite of the fact that here the spin conservation rule is violated. Thus, a function of total angular momentum must be employed to represent the mercury

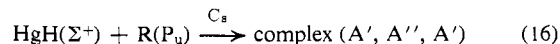
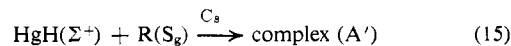
(13) In estimating  $\sigma_{\text{chem}}$  for CH<sub>3</sub>CD<sub>2</sub>CH<sub>3</sub>, complications arising from the fact that the intercept may be slightly higher than unity are not taken into account. True initial slope may give a somewhat higher  $\sigma^2_{\text{chem}}$  for this compound.

orbital. Such an approach was first tested in the quenching of Hg\* by N<sub>2</sub> with a satisfactory result.<sup>14</sup>

In the present work, we assume the following model. An excited mercury atom, with a definite  $J$  value, forms a planar complex<sup>15a</sup> with a paraffin which is approximated as a diatom, RH; the H atom to which R and mercury are bound is supposed to come from the weakest bond in the paraffin.<sup>15b</sup> In the quenching of Hg\*(<sup>3</sup>P<sub>1</sub>) atoms, a total cross section for a molecule can often be estimated by simply adding the contribution from each bond.<sup>3</sup> This suggests as an approximation that, in the quenching, each bond behaves independently of the other; one is then justified to regard a paraffin as a perturbed diatom, CH, as is done in the above model. This is a crude approximation. It is, however, a very useful one, and provides some illuminating results on the basis of symmetry arguments.<sup>16,17</sup> For the quenching reaction to proceed readily, a state of the complex arising from the reactant side and a state of the complex arising from the product side must belong to the same symmetry species. In C<sub>s</sub> symmetry, to which the present planar complex belongs, Hg\*(<sup>3</sup>P<sub>1</sub>) with a  $J$  value of unity gives three states of A', A'', and A' species, while Hg\*(<sup>3</sup>P<sub>0</sub>) with a  $J$  value of zero provides a single state of A' species.<sup>18</sup> Since the Σ<sup>+</sup> ground state of RH becomes an A' state, we obtain



To obtain the symmetry species involved in reaction 5, we use the result of theoretical work<sup>17,19</sup> on the linear Hg\*-H<sub>2</sub> system, which indicates that, in reaction 5 with H<sub>2</sub>, HgH is produced in the Σ<sup>+</sup> state and subsequently dissociates to give Hg and H. Since R may be approximated as having an electron in an s orbital or an electron in a p orbital, we have



The comparison of (14) with (15) and (16) indicates that the quenching of metastable atoms to ground state is allowed if R has p character; but, as is in the quenching by H<sub>2</sub>, if R can only be in S state, the transition is forbidden. On the other hand, the quenching of Hg\* atoms is allowed, regardless of the state of R. In view of hybridization in the alkyl radical, R involved in paraffin quenching should be considered as an atom with a state between S<sub>g</sub> and P<sub>u</sub>. The quenching of Hg' is thus partly allowed. One then expects that, com-

(14) V. K. Bykhovskii and E. E. Nikitin, *Opt. Spectry.*, **16**, 111 (1964).

(15) (a) The present planar complex involving a H<sub>2</sub> molecule is a generalization of a cyclic complex proposed in ref 10. With paraffins, the present complex is essentially a bent triatomic molecule, because R-Hg interaction is expected to be much weaker than Hg-H interaction. (b) Even though an excited mercury atom does not always complex at the most weakly bonded H, experimental data indicate that the interaction with the weakest CH is the most important process; see, for example, ref 3, and R. A. Holroyd and G. W. Klein, *J. Phys. Chem.*, **67**, 2273 (1963).

(16) K. E. Shuler, *J. Chem. Phys.*, **21**, 624 (1953).

(17) K. J. Laidler, "The Chemical Kinetics of Excited States," Clarendon Press, Oxford, 1955, pp 172-174.

(18) G. Herzberg, "Molecular Spectra and Molecular Structure. III. Electronic Spectra and Electronic Structure of Polyatomic Molecules," D. Van Nostrand Co., Inc., New York, N. Y., 1966.

(19) K. J. Laidler, *J. Chem. Phys.*, **10**, 43 (1942).

pared with  $\text{Hg}^*$ ,  $\text{Hg}'$  atoms should be less reactive but not negligibly so. Experimental data show  $\text{Hg}'$  atoms to be about 20 times less reactive. In quenching by  $\text{H}_2$ , however, the quenching of  $\text{Hg}'$  to the ground state is forbidden; hence, here  $\text{Hg}'$  atoms should be very much less reactive than  $\text{Hg}^*$ . Experimental data indicate  $\text{Hg}'$  atoms are about 600 times less reactive.<sup>5,20</sup>

To discuss the quenching of  $\text{Hg}^*$  to  $\text{Hg}'$ , it is necessary to consider the stability of electronic states. In one of the  $A'$  types, the positive lobe of the mercury orbital points toward the RH orbital (which has positive sign), while the negative lobe points away. This state should be attractive. In the other  $A'$  type, the negative lobe points to the RH orbital, and the state is repulsive. In  $A''$  symmetry, however, both negative and positive lobes are about the same distance away from the RH orbital; this state cannot be bonding. Thus, it is evident that only one of the  $A'$  states leads to the formation of a strongly coupled collision complex. We assume that this state is involved in the quenching. The quenching of  $\text{Hg}^*$  to  $\text{Hg}'$  is then forbidden unless vibrational or rotational motion is excited. All the vibrational states in the present triatomic complex belong to the  $A'$  species<sup>21</sup> and cannot induce the  $A'-A''$  transition. The rotation around the two axes in the symmetry plane, however, belongs to the  $A''$  type; hence, the transition can be induced by this motion. When this rotationally excited complex decomposes, it should produce the rotationally excited RH. The recent phase space theory of reaction rate<sup>22</sup> indicates that, in the above quenching by rotational excitation, the cross section increases with decreasing spacing of rotational energy levels in RH. When H in RH is replaced by D, the rotational spacing decreases by nearly half, but deuteration of the alkyl group decreases the spacing only slightly. Recalling that H in RH comes from the weakest bond, we conclude that the deuteration at the weakest bond increases the rate of  $\text{Hg}'$  formation, while this rate is affected very little by the deuteration at other bonds. Qualitatively, this is in agreement with experimental observations.<sup>1</sup>

It has been customary to suppose that the quenching of  $\text{Hg}^*$  to  $\text{Hg}'$  proceeds by the vibrational excitation of RH.<sup>23,24</sup> This supposition is often used together with the resonance-energy rule according to which the quenching occurs most readily when the vibrational energy spacing is the closest to the energy difference ( $1768\text{ cm}^{-1}$ ) between  $\text{Hg}^*$  and  $\text{Hg}'$ . This view does not agree with experiments. The cross section for  $\text{CH}_3\text{CD}_2\text{CH}_3$  contains a large contribution from the quenching to the metastable state, but it shows negligible temperature dependence. Thus, the quenching is either thermoneutral or exothermic. In propane, the vibrational frequencies assigned to the  $\text{CH}_2$  group are<sup>25</sup> 940, 1278, 1338, and 1460 and doubly degenerate 2950  $\text{cm}^{-1}$ . Hence, one must assume that the  $1460\text{-cm}^{-1}$

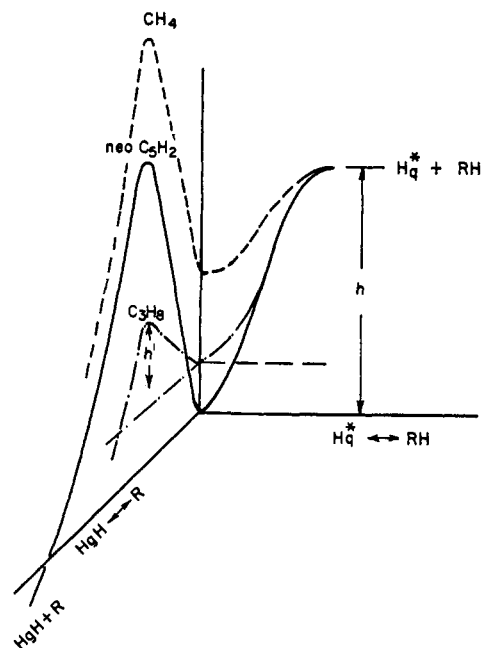


Figure 6. Potential diagram for a planar complex between  $\text{Hg}^*$  and RH.

vibration is excited. Deuteration reduces this frequency, and the discrepancy from the resonance value of  $1768\text{ cm}^{-1}$  increases. Thus, deuteration should decrease the formation of  $\text{Hg}'$  atoms. This is not true.

To explain the abnormal behavior of neopentane, it is now necessary to explore the factors which affect the lifetime,  $\tau_c$ , of the complex. Since reaction 5 involves the breaking of a CH bond, motion along this reaction coordinate is likely to encounter a potential barrier. This situation is schematically shown in Figure 6, where the height of this barrier is denoted  $h'$ . In free-radical reactions involving a bond breakage, it is often found that activation energies increase with increasing bond strengths and also that a small fractional difference in bond strength leads to a large fractional difference in activation energy. A potential model used to explain this fact can also be used in the present case to demonstrate that  $h'$  increases with increasing bond strength, and also that a small difference in bond energy induces a large fractional change in  $h'$ . Since bond energy increases in the order<sup>26</sup>  $i\text{-C}_4\text{H}_{10}$ ,  $\text{C}_3\text{H}_8$ ,  $\text{C}_2\text{H}_6$ ,  $\text{C}(\text{CH}_3)_4$ ,  $\text{CH}_4$ , this must be the order with which  $k_5$  sharply decreases. Another factor which is important in discussing  $\tau_c$  is the energy difference between the complex and reactant state. This is denoted  $h$  in Figure 6. Here,  $h$  is likely to increase with increasing polarizability of R, which is essentially the same as the polarizability of a paraffin, because then a stronger bond is expected to form between R and  $\text{Hg}^*$ . Hence,  $k_{-2}$ , which increases with decreasing depth of  $h$ , must increase in the order  $\text{C}(\text{CH}_3)_4$ ,  $i\text{-C}_4\text{H}_{10}$ ,  $\text{C}_3\text{H}_8$ ,  $\text{C}_2\text{H}_6$ ,  $\text{CH}_4$ . On the basis of these arguments, potential surfaces involved in the quenching by  $\text{C}_3\text{H}_8$ ,  $\text{C}(\text{CH}_3)_4$ , and  $\text{CH}_4$  are schematically depicted as shown in Figure 6. In  $\text{CH}_4$ ,  $h$  is very shallow but  $h'$  is very high; hence, the maximum in the plane representing the plot of  $\text{HgH-R}$  against the energy plane may lie considerably higher than the energy of the reactants,

(20) The quenching cross section for  $\text{Hg}^*$  given in ref 5 is about two times too low; see ref 11.

(21) G. Herzberg, "Infrared and Raman Spectra," D. Van Nostrand Co., Inc., New York, N. Y., 1945, p 134.

(22) P. Pechukas, J. C. Light, and C. Rankin, *J. Chem. Phys.*, **44**, 794 (1966).

(23) P. G. Dickens, J. W. Linnett, and O. Sovers, *Discussions Faraday Soc.*, **33**, 52 (1962).

(24) A. C. G. Mitchell and M. W. Zemansky, "Resonance Radiation and Excited Atoms," The Cambridge University Press, Cambridge, 1961.

(25) K. S. Pitzer, *J. Chem. Phys.*, **12**, 310 (1944).

(26) J. A. Kerr, *Chem. Rev.*, **66**, 465 (1966).

as indicated in Figure 6. If so,  $\phi(H)$  at room temperature should be very small, but at high temperature,  $\phi(H)$  should become appreciable. This agrees with experimental observations. There are two other constants,  $k_3$  and  $k_4$ , affecting  $\tau_c$ . Nothing is known about these constants, but these are likely to be affected by the change in bond strength or polarizability as much as  $k_5$  and  $k_2$  are affected. We hence assume that  $k_3$  and  $k_4$  for various RH are about the same. The difference in lifetime among paraffins is then governed by  $k_5$  and  $k_2$ . In all paraffins of present concern except neopentane, high  $h'$  is accompanied by a shallow  $h$ . Neopentane is unusual in that  $h'$  is high, while  $h$  is very deep. According to the present argument, then, neopentane should have the longest  $\tau_c$ . Since the rates of reactions 3 and 4 are proportional to  $\tau_c$ , one can thus rationalize at least qualitatively the fact that neopentane shows abnormally high light emission and also the fact that neopentane is the only undeuterated paraffin which produces detectable Hg' atoms.

**Acknowledgment.** Mr. J. D. Reedy helped with the experiments, and Mr. C. L. Hassell offered valuable suggestions. This assistance is gratefully acknowledged.

### Appendix

Table III shows that  $\alpha/\beta$  decreases sharply when temperature increases. At first sight, this may seem surprising. An attempt is hence made in this Appendix to treat this phenomenon in some detail. As shown in (IV),  $\alpha/\beta$  is the product of  $k_2\tau_c(k_4 + k_5)$  and  $(ck_1)^{-1}$ . When expressed in  $\text{mm}^{-1} \text{sec}^{-1}$ ,  $k_2\tau_c(k_4 + k_5)$  decreases with  $T^{-1/2}$ . The other factor,  $(ck_1)^{-1}$ , is the average time,  $\tau$ , the photon spends (as Hg\*) in the cell. In the present experiment, the pressure of mercury is high ( $1.2 \times 10^{-3}$  torr), and the fluorescent light becomes absorbed several times before it escapes from the cell. Hence,  $\tau$  is much larger than  $\tau_0$ , the mean life of an isolated atom ( $1.08 \times 10^{-7}$  sec). Milne<sup>27</sup> derives an equation for  $\tau$  which at high opacities ( $=k\rho$ ) becomes

$$\frac{\tau}{\tau_0} = 1 + \frac{4}{\pi^2} (k\rho)^2 \quad (\text{X})$$

(27) E. A. Milne, *J. London Math. Soc.*, 1, 1 (1926).

where  $k$  is the absorption coefficient and  $\rho$  is the distance the photon traverses before escaping from the cell. Milne's theory has defects,<sup>27</sup> but it is simple and agrees well with experimental observations at low opacities.<sup>11</sup> For the moment, we assume that  $k$  is the same as the absorption coefficient,  $k_0$ , at the center of the Doppler broadened absorption line. Then  $k_0 = (2.59 \times 10^4)T^{-3/2}$  at a mercury vapor pressure of  $1.2 \times 10^{-3}$ . Hence,  $k_2\tau_c(k_4 + k_5)/(ck_1)$  decreases approximately with  $T^{-3.5}$ . A successful approximation for  $k$  at low opacities is<sup>11</sup>

$$e^{-k\rho} = T(\rho) \quad (\text{XI})$$

where  $T(\rho)$  is the properly averaged probability that the photon traverses a distance  $\rho$  without being absorbed. An approximate equation for  $T(\rho)$  to be used at high opacities is<sup>28</sup>

$$T(\rho) = \frac{1}{k_0\rho(\pi \ln k_0\rho)^{1/2}} \quad (\text{XII})$$

Table VI compares theoretical  $\tau/\tau_0$ , calculated with

**Table VI.<sup>a</sup>** Effect of Imprisonment on Mean Life

Temp, °C	$(\tau/\tau_0)_{\text{obsd}}$	$(\tau/\tau_0)_{\text{calcd}}$
25	10.7	5.9
125	4.1	4.1
202	2.8	3.1

<sup>a</sup>  $\tau$  = imprisonment lifetime,  $\tau_0$  = mean life of an isolated Hg\*(<sup>3</sup>P<sub>1</sub>) atom.

eq X-XII, with experimental  $\tau/\tau_0$ 's obtained from  $\alpha/\beta$  values. At 202 and 125°, agreement is good; but at 25°, where  $k_0\rho$  is the highest, the calculated value is too low. The above argument nevertheless shows that Milne's theory provides at least a qualitative explanation for the sharp temperature dependence of the slope of the modified Stern-Volmer formula observed in Figures 1 and 2.

(28) T. Holstein, *Phys. Rev.*, 72, 1212 (1947).